

Calcium Channel Block by (-)Devapamil Is Affected by the Sequence Environment and Composition of the Phenylalkylamine Receptor Site

V. E. Degtiar,* S. Aczél,* F. Döring,* E. N. Timin,# S. Berjukow,* D. Kimball,§ J. Mitterdorfer,* and S. Hering*

*Institut für Biochemische Pharmakologie, A-6020 Innsbruck, Austria; #A. V. Vishnevsky Institute of Surgery, 113 039 Moscow, Russia; and §Bristol-Myers Squibb Pharmaceutical Company, Princeton, New Jersey 08543-4000 USA

ABSTRACT The pore-forming α_1 subunit of L-type calcium (Ca^{2+}) channels is the molecular target of Ca^{2+} channel blockers such as phenylalkylamines (PAAs). Association and dissociation rates of (-)devapamil were compared for a highly PAA-sensitive L-type Ca^{2+} channel chimera (L_h) and various class A Ca^{2+} channel mutants. These mutants carry the high-affinity determinants of the PAA receptor site in a class A sequence environment. Apparent drug association and dissociation rate constants were significantly affected by the sequence environment (class A or L-type) of the PAA receptor site. Single point mutations affecting the high-affinity determinants in segments IVS6 of the PAA receptor site, introduced into a class A environment, reduced the apparent drug association rates. Mutation I1811M in transmembrane segment IVS6 (mutant AL25/-I) had the highest impact and decreased the apparent association rate for (-)devapamil by ~30-fold, suggesting that this pore-lining isoleucine in transmembrane segment IVS6 plays a key role in the formation of the PAA receptor site. In contrast, apparent drug dissociation rates of Ca^{2+} channels in the resting state were almost unaffected by point mutations of the PAA receptor site.

GLOSSARY

B_N	fraction of blocked channels after the N th pulse
B_∞	steady level of the current inhibition
(-)-dev	(-)-devapamil
[D]	drug concentration
$g_{\text{Ca}}(t)$	fraction of open channels
$g_{\text{peak, max}}$	maximum value of g_{peak}
I_{Ba}	barium inward current through Ca^{2+} channels
I_t	peak current values in drug at a given time (t) after a train
I_{15}	peak current values of the 15th conditioning pulse
I_0	peak current values in absence of drug
I_{ss}	steady (noninactivating) current component
I_{peak}	peak current value
$k_1[\text{D}]$	apparent first-order association rate constant
k_1	apparent second-order association rate constant
k_{-1}	apparent dissociation rate constant
q(-)dev	q(-) devapamil; quaternary derivative of (-)devapamil
T	period of stimulation

Greek symbols

τ_{block}	time constant of peak current inhibition during a train
τ_{rec}	time constant of recovery from block at rest

INTRODUCTION

The pore-forming α_1 subunit of L-type Ca^{2+} channels (classes C(α_{1C}), D(α_{1D}), and S(α_{1S})) is the molecular target of Ca^{2+} channel blockers such as phenylalkylamines (PAAs). L-type Ca^{2+} channels have much higher affinity for PAAs compared to other classes (A(α_{1A}), B(α_{1B}), and E(α_{1E})) (Glossmann and Striessnig, 1990; Catterall and Striessnig, 1992; Birnbaumer et al., 1994; Hofmann et al., 1994; Catterall, 1995; Dunlap et al., 1995; Ishibashi et al., 1995; Diochot et al., 1995). The action of PAAs on L-type Ca^{2+} channels is crucially dependent on the open-channel conformation (Lee and Tsien, 1983; McDonald et al., 1994; Hering et al., 1989; Timin and Hering, 1992). A major step toward an understanding of the molecular mechanism of high-affinity PAA interaction with L-type Ca^{2+} channels was made by Hockerman et al. (1995), who systematically mutated transmembrane segment IVS6 of the α_{1C} subunit and identified three putative pore-oriented amino acids (Tyr-1463, Ala-1467, Ile-1470, numbering according to α_{1C-c} ; Hockerman et al., 1995) as molecular determinants of the PAA receptor site. High PAA sensitivity can be generated for class A Ca^{2+} channels by transferring the IVS6 segment of L-type α_{1S} to α_{1A} , accordingly (Döring et al., 1996). Furthermore, we have recently demonstrated that replacement of as few as three amino acids in transmembrane segment IVS6 of the α_{1A} subunit by the respective L-type residues (I1804Y, S1808A, and M1811I, chimera AL25; α_{1A} numbering) is sufficient to support use-dependent block by (-)gallopamil. Transfer of only part of the L-type PAA receptor site to α_{1A} induced a less pronounced use-dependent Ca^{2+} channel block (Hering et al., 1996).

In the present paper we expressed the L-type Ca^{2+} channel construct L_h and various α_{1A} mutants containing either the high-affinity PAA receptor site of L-type Ca^{2+} channels in transmembrane segment IVS6 (mutant AL25; Hering et al., 1996) or only part of it (mutants AL25/-Y, AL25/-A,

Received for publication 15 October 1996 and in final form 10 April 1997.

Address reprint requests to Dr. Steffen Hering, Institut für Biochemische Pharmakologie, Peter-Mayr-Straße 1, A-6020 Innsbruck, Austria. Tel.: ++43-512-507-3154; Fax: ++43-512-588627.

© 1997 by the Biophysical Society

0006-3495/97/07/157/11 \$2.00

AL25/-I) together with β_{1a} and $\alpha_{2-\delta}$ subunits in *Xenopus* oocytes (Grabner et al., 1996). We performed a quantitative analysis of the apparent PAA association and dissociation rates of the PAA (-)devapamil by means of a previously described technique (Timin and Hering, 1992). Our results demonstrate that the apparent PAA-Ca²⁺ channel association and dissociation rates are not only affected by single point mutations of the putative PAA receptor site, but by its sequence environment as well (α_{1A} or α_{1C}).

MATERIALS AND METHODS

Electrophysiology

Inward barium currents were studied with two-microelectrode voltage-clamp of *Xenopus* oocytes after microinjection of cRNAs (2–7 days) in approximately equimolar mixtures of α_1 (0.3 ng/50 nl)/ β_{1a} (16) (0.1 ng/50 nl)/ $\alpha_{2-\delta}$ (17) (0.2 ng/50 nl) as previously described (Grabner et al., 1996; Hering et al., 1996). All experiments were carried out at room temperature in a bath solution with the following composition: 40 mM Ba(OH)₂, 40 mM *N*-methyl-D-glucamine, 10 mM HEPES, 10 mM glucose (pH adjusted to 7.4 with methanesulfonic acid). Voltage-recording and current injecting microelectrodes were filled with 2.8 M CsCl, 0.2 M CsOH, 10 mM EGTA, and 10 mM HEPES (pH 7.4) and had resistances of 0.3–2 M Ω . Activation of endogenous Ca²⁺-activated Cl⁻ conductance by barium influx through Ca²⁺ channels was eliminated by injecting the oocytes 20–40 min before the voltage-clamp experiments with 50–100 nl of a 0.1 M 1,2-bis(2-aminophenoxy)ethane-*N,N,N,N*-tetraacetic acid solution. Peak I_{Ba} amplitudes of the expressed channel constructs ranged from 200 to more than 5 μ A. Oocytes with current amplitudes that were larger than 2 μ A were excluded from the analysis.

The recording chamber (150 μ l total volume) was continuously perfused at a flow rate of 1 ml/min with control or drug-containing solutions. Data were digitized at 2 kHz, filtered at 0.5 kHz, and stored on a computer hard disk. We used the pClamp software package (version 6.0; Axon Instruments) for data acquisition and analysis. Leakage current correction was performed by using average values of scaled leakage currents elicited by a 10-mV hyperpolarizing voltage step.

Intracellular application of (-)q-devapamil

The intracellular action of the quaternary derivative of (-)devapamil, (-)q-devapamil, was studied by microinjecting 50 nl of a 1 mM solution of (-)q-devapamil (dissolved in distilled water) into oocytes expressing chimeras L_h and AL25. Assuming an average oocyte volume of 0.5 μ l, we calculated an intracellular concentration of 100 μ M.

Estimation of association and dissociation rate constants to open Ca²⁺ channels

Use-dependent block of I_{Ba} by (-)devapamil was studied during 15 subsequent test pulses of different lengths applied at a standard frequency of 0.1 Hz from -80 mV holding potential to a test potential of 20 mV. The oocytes were held for 15–25 min (depending on the batch of oocytes) at -80 mV until I_{Ba} was stable. I_{Ba} of class A mutants were stable under voltage-clamp conditions up to 3 h; I_{Ba} "run-down" was negligible. To evaluate the peak I_{Ba} decay under control conditions, we applied identical test pulse sequences in the absence of drug. PAA effects on I_{Ba} were studied after a 3-min equilibrium period in drug-containing solution. Tonic ("resting-state dependent") block after a 3-min equilibration in 50 μ M (-)devapamil containing solution was usually less than 10% (Hering et al., 1996).

The method for estimation of apparent association and dissociation rate constants from the kinetics of use-dependent inhibition of Ca²⁺ channels was previously described in detail (Timin and Hering, 1992). Rate constant k_1 describes drug association with open Ca²⁺ channels. We did not distinguish between drug dissociation from different channel states (open/closed) and estimated a single dissociation time constant k_{-1} reflecting drug dissociation from open as well as from closed channel states. Drug-bound channels were postulated to be not conducting.

The kinetic equation (see also Starmer and Grant, 1985) is

$$\frac{dB}{dt} = k_1[D] \cdot g_{Ca}(t) \cdot (1 - B) - k_{-1} \cdot B$$

where B equals the fraction of blocked channels, $g_{Ca}(t)$ the fraction of open channels, $[D]$ the concentration of drug, and k_1 and k_{-1} the apparent association and dissociation rate constants, respectively. The solution of the above equation predicts an exponential increase in the fraction of blocked channels during a train:

$$B_N = B_\infty [1 - \sigma^N(T)]$$

where B_N is the fraction of blocked channels after the N th pulse, B_∞ is the steady level of the current blockade, and T is the period of stimulation. The parameters of the current blockade in a train (σ and B_∞) were determined from experimental data by a least-squares analysis. The solution of the kinetic equation links the parameters of the blockade in train with the apparent first-order rate constants $k_1[D]$ and k_{-1} .

$$k_1[D] = \frac{\ln(1 + \Phi(T))}{\int_0^{t_{imp}} g_{Ca}(t) dt}$$

$$k_{-1} = -\ln\{\sigma(T)[1 + \Phi(T)]\}/T$$

where

$$\Phi(T) = \frac{B_\infty [1 - \sigma(T)]}{\sigma(T)}$$

An appropriate software (USE-DEP) was developed. The following values were utilized for estimation of the apparent rate constants: 1) peak current values, 2) individual current time integrals of a given train (15 pulses), and 3) period of pulse application. Current traces were processed by means of the software pCLAMP (Axon Instruments), thereby creating files for the USE-DEP software. The statistical significance of I_{Ba} block by (-)devapamil was calculated according to an unpaired Student's *t*-test. Data are given as mean \pm SD.

Molecular biology

The construction of chimera L_h (repeats I–IV from α_{1C-a} ; Mikami et al., 1989), N-terminus replaced by the corresponding sequences from carp skeletal muscle α_{1S} (Grabner et al., 1991), was previously described (Döring et al., 1996; Grabner et al., 1996; Hering et al., 1996). Chimera AL25 and its derivatives AL25/-Y, AL25/-A, and AL25/-I (Hering et al., 1996) were constructed by introducing point mutations into α_{1A} cDNA (Mori et al., 1991) by the "gene SOEing" technique (Horton et al., 1989). AL30 was generated by applying the same procedure to introduce five point mutations (Y1386I, M1387F, A1390S, I1393M, I1394L; amino acid numbering according to carp skeletal muscle α_{1S} ; Grabner et al., 1991) into chimera AL23. Construction of AL23 was described in detail (Döring et al., 1996). Polymerase chain reaction (PCR) was performed using proof-reading Pfu-polymerase (Stratagene), and fused SOE-cDNAs were inserted into the *KpnI* (nucleotide 5467)-*BglIII* (nucleotide 6185) cassette of chimera

AL22 (Döring et al., 1996). Chimeric constructs were verified by sequence analysis (Sanger et al., 1977).

RESULTS

Apparent association and dissociation rates of (–)de vapamil for the L-type chimera L_h and the PAA-sensitive class A Ca²⁺ channel mutant AL25

To evaluate the influence of the sequence environment of the PAA receptor on the kinetics of Ca²⁺ channel block, we expressed chimeras L_h (Grabner et al., 1996) and the class A Ca²⁺ channel mutant AL25 (Hering et al., 1996) in *Xenopus* oocytes. Mutant AL25 was constructed by transferring the putative high-affinity determinants of the L-type PAA receptor site (Hockerman et al., 1995) to transmembrane segment IVS6 of α_{1A} (mutations I1804Y, S1808A, and M1811I; Hering et al., 1996).

Fig. 1 displays current traces of chimeras L_h and AL25 evoked by pulses from a holding potential of –80 mV to a test potential of 20 mV in the presence of 50 μ M (–)de vapamil. Prolongation of the test pulse accelerated the block development and induced a more pronounced current inhibition in steady state. The current inhibition at a given pulse length (50, 100, or 800 ms) developed faster in chimera AL25 (Fig. 1). A comparison of the first-order apparent rate constants ($k_1[D]$, k_{-1}) of mutant AL25 and chimera L_h is given in Table 1. Compared to chimera L_h, the apparent drug association and dissociation rates were significantly higher in mutant AL25. Prolongation of the test pulse from 50 to 800 ms (Table 1) did not significantly affect the apparent drug association rate, although the main characteristics of the current inhibition (time constant of peak current decay, steady-state level of block) differed notably for both channel constructs (Fig. 1). As expected, association but not drug dissociation rate was dependent on the applied drug concentration (Table 2).

Drug dissociation from chimera L_h and mutant AL25 in the resting state

The dissociation rate of (–)de vapamil with resting Ca²⁺ channels can be estimated by studying the recovery of Ca²⁺ channels from use-dependent block by applying an additional test pulse after different time intervals after the conditioning pulse train. The estimation of PAA dissociation rates from resting Ca²⁺ channels at a holding potential of –80 mV is illustrated in Fig. 2. Between subsequently applied trains, the membrane was held for 3 min at –100 mV to remove block by (–)de vapamil (Fig. 2). *I*_{Ba} of AL25 recovered at a holding potential of –80 mV from block within ~4 min, whereas *I*_{Ba} of L-type chimera L_h at the same potential did not completely recover, even within 8 min, indicating that the estimated recovery time constant (Fig. 2 and Table 2) reflects only the fast kinetic component of drug dissociation at this potential. We were, however,

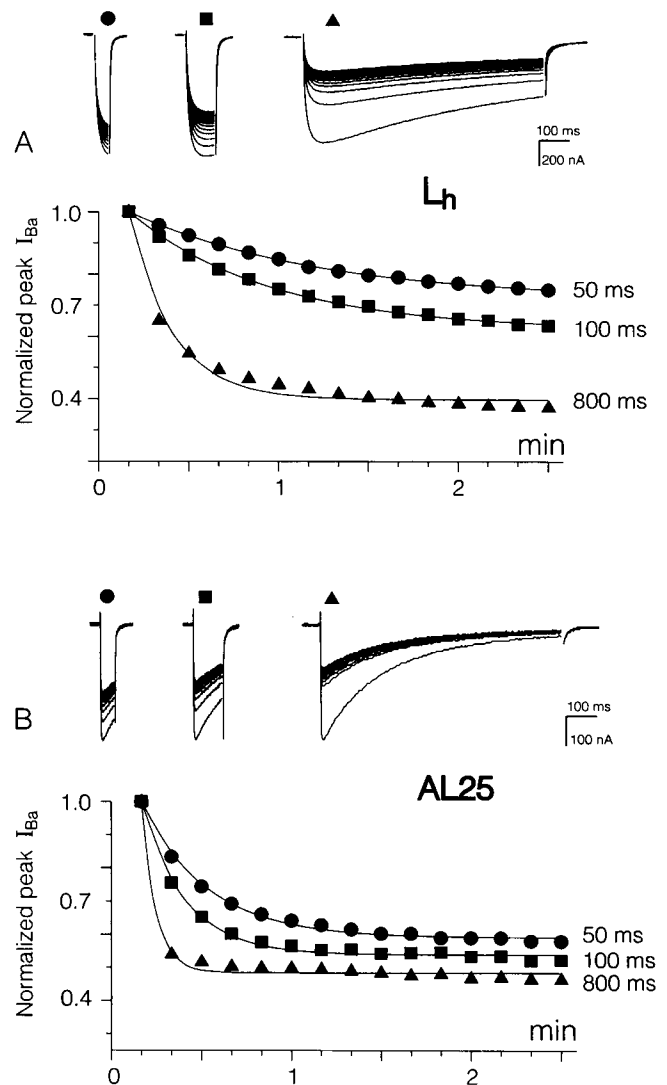


FIGURE 1 Use-dependent *I*_{Ba} block by (–)de vapamil during trains of test pulses in oocytes expressing chimera L_h and mutant AL25. (A) Peak *I*_{Ba} amplitudes of L_h during 15 consecutive depolarizing voltage pulses applied from the holding potential of –80 to 20 mV at 0.1 Hz in the presence of 50 μ M (–)de vapamil. The pulse durations were 50 ms (●), 100 ms (■), and 800 ms (▲). *I*_{Ba} amplitudes were normalized to the amplitude of *I*_{Ba} elicited by the first pulse in a train. Corresponding *I*_{Ba} recordings are shown in the top of the panel. (B) Use-dependent peak *I*_{Ba} decay in the presence of 50 μ M (–)de vapamil of mutant AL25. Pulse protocol and symbols are the same as in A. Data were fitted by single-exponential functions $I_{ss} - (I_{ss} - I_{peak}) \exp(-t/\tau_{block})$, yielding the following steady-state levels and time constants (I_{ss} , τ_{block} (s)): L_h: ●, 0.72 and 62 s; ■, 0.62 and 46 s; ▲, 0.4 and 14 s; AL25: ●, 0.59 and 21 s; ■, 0.54 and 14 s; ▲, 0.48 and 5 s.

unable to resolve the kinetics of the slow component of *I*_{Ba} recovery from block in L_h, because a contamination by current rundown during longer lasting measurements could not be excluded. Complete unblock of L_h was, however, achieved at more negative holding potentials (–100 to –120 mV), indicating a voltage dependence of drug dissociation (data not shown).

TABLE 1 Apparent first-order association (k_1 [D]) and dissociation (k_{-1}) rate constants of (-)devapamil (50 μ M) interaction with chimera L_h and mutant AL25 estimated for different test pulse length

Test pulse length (ms)	L_h		AL25	
	k_1 [D] (s^{-1})	k_{-1} (s^{-1})	k_1 [D] (s^{-1})	k_{-1} (s^{-1})
20			6.5 ± 1.56 ($n = 3$)	0.023 ± 0.0017 ($n = 3$)
50	1.62 ± 0.55 ($n = 4$)	0.013 ± 0.0013 ($n = 4$)	6.3 ± 1.56 ($n = 3$)	0.025 ± 0.0005 ($n = 3$)
100	1.1 ± 0.4 ($n = 4$)	0.012 ± 0.006 ($n = 4$)*	6.2 ± 1 ($n = 4$)	0.026 ± 0.002 ($n = 4$)*
200			6.5 ± 1.73 ($n = 3$)	0.029 ± 0.0017 ($n = 3$)
400			4.6 ± 2.2 ($n = 3$)	0.030 ± 0.0008 ($n = 3$)
800	1.0 ± 0.3 ($n = 4$)	0.017 ± 0.006 ($n = 4$)*	5.6 ± 1 ($n = 4$)	0.031 ± 0.004 ($n = 4$)*

*Significantly different for experiments performed with 100-ms and 800-ms long test pulses ($p < 0.05$). Conditioned block of I_{Ba} was measured during trains of 15 consecutive depolarizing voltage pulses (100 ms, 0.1 Hz). Values are given as mean \pm SD (n , number of experiments).

Molecular determinants of the PAA receptor site in transmembrane segment IVS6 affect apparent association rate for (-)devapamil

Three amino acids form the putative high-affinity binding site for PAAs in L-type Ca^{2+} channels (Hockerman et al., 1995). If only two out of three amino acids are transferred from α_{1S} to α_{1A} , the sensitivity of the resulting mutants for the PAA (-)gallopamil is significantly reduced (Hering et al., 1996). We made a similar observation for the block of α_{1A} -derived Ca^{2+} channel mutants by (-)devapamil. Compared to chimera AL25 that carried three high-affinity determinants of the PAA receptor site, the steady level of block by (-)devapamil was reduced when one of the high-affinity determinants was replaced by the corresponding amino acid of the α_{1A} subunit (Tyr replaced by Ile in AL25/-Y, Ala by Ser in AL25/-A, and Ile by Met in AL25/-I) (see Table 3). The kinetics of I_{Ba} block by 50 μ M (-)devapamil during a 0.1-Hz pulse train (100 ms) of mutants AL25, AL25/-Y, AL25/-A, and AL25/-I are compared in Fig. 3 A and B. As expected, the fastest development of block was observed for mutant AL25 carrying all three amino acids of the putative PAA receptor site. Substitutions Y1804I and A1808S, yielding mutants AL25/-Y and AL25/-A, respectively, slowed the kinetics of block development and additionally exhibited a reduced steady level of block (Table 3). The most dramatic reduction in block development occurred after substitution of I1811M in AL25, resulting in mutant AL25/-I. The corresponding ap-

TABLE 2 Concentration dependence of apparent first-order association (k_1 [D]) and dissociation (k_{-1}) rate constants of (-)devapamil (Dev) with chimera L_h and mutant AL25

[Dev]		L_h	AL25
5 μ M	k_1 [D] (s^{-1})	0.3 ± 0.16 ($n = 7$)	1.4 ± 0.55 ($n = 18$)*
50 μ M	k_1 [D] (s^{-1})	1.1 ± 0.38 ($n = 10$)	5.5 ± 1.45 ($n = 25$)*
5 μ M	k_{-1} (s^{-1})	0.012 ± 0.008 ($n = 7$)	0.026 ± 0.0085 ($n = 18$)*
50 μ M	k_{-1} (s^{-1})	0.015 ± 0.0064 ($n = 10$)	0.032 ± 0.03 ($n = 25$)*
50 μ M	τ_{rec} (s)	106 ± 22 ($n = 4$)	67 ± 12.1 ($n = 3$)

Values are given as mean \pm SD (n , number of experiments).

*Values for L_h and AL25 differ significantly ($p < 0.05$).

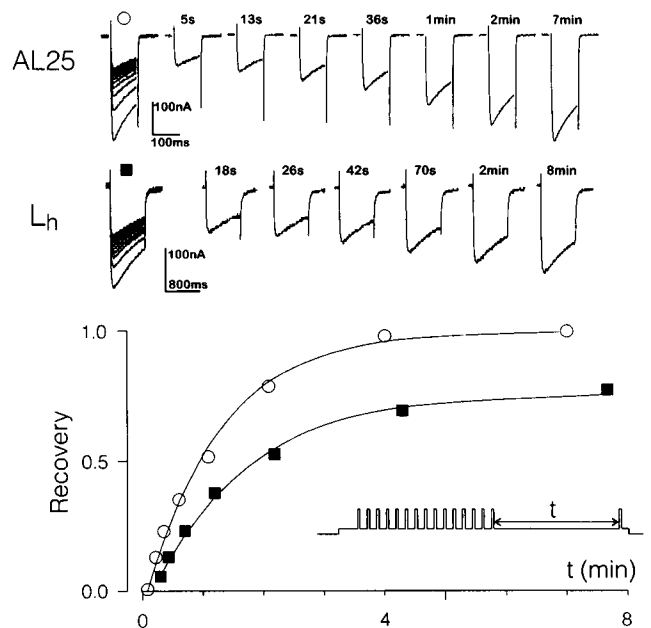


FIGURE 2 Recovery of I_{Ba} from block induced by 15 subsequently applied pulses from -80 mV to 20 mV in the presence of 50μ M (-)devapamil in oocytes expressing chimera L_h and mutant AL25. To increase the amount of peak I_{Ba} inhibition during the conditioning train, the pulse length during I_{Ba} measurements of L_h was extended to 800 ms. Recovery reflects mainly channel unblock, because less than 5% ($n = 5$) of the peak I_{Ba} of L_h and $12 \pm 5\%$ ($n = 4$) of AL25 accumulated in an inactivated state during the pulse train in control. (Upper panels) I_{Ba} records illustrating current recovery from block. Superimposed traces of I_{Ba} during trains (100 ms, 0.2 Hz for AL25, or 800 ms, 0.1 Hz for L_h) and single traces recorded at different times after a train are displayed. (Lower panel) Normalized peak I_{Ba} corresponding to currents shown in the upper panel. The applied pulse protocol is displayed in the inset. Extent of recovery from block was calculated as $\text{Recovery} = (I_t - I_{15}) / (I_0 - I_{15})$, where I_t is the peak current value in drug at a given time (t) after a train, I_{15} is the peak current value of the 15th conditioning pulse (maximum block); I_0 is the peak current value in absence of drug. Curves represent single-exponential fits ($\text{Recovery} = C * \{1 - \exp(-t/\tau_{rec})\}$). Parameters of fit (AL25, \circ): $C = 1$, $\tau_{rec} = 73$ s; L_h , \blacksquare): $C = 0.76$, $\tau_{rec} = 96$ s. Between the subsequently applied pulse trains the membrane voltage was held for 3 min at -100 mV, resulting in complete unblock of the channels. I_{Ba} of mutant AL25 recovered by up to 100% of its initial value, whereas recovery of chimera L_h at the same holding potential was incomplete (range 0.60 – 0.85). Prolonged hyperpolarization at -100 mV consistently induced 100% recovery from use-dependent block of L_h .

TABLE 3 Use-dependent inhibition of I_{Ba} by (-)devapamil in mutants AL25, AL25/-Y, AL25/-A, and AL25/-I and apparent dissociation rate constants

		Peak current inhibition			
		AL25	AL25/-Y	AL25/-A	AL25/-I
Contr.		8 ± 3.1% (n = 15)	9.3 ± 0.6% (n = 3)	7.2 ± 3.6% (n = 5)	4.5 ± 2 (n = 4)
Dev	5 μM	24 ± 7.2% (n = 13)	10.6 ± 1.6% (n = 3)	12 ± 5.2% (n = 3)	5.6 ± 2.9% (n = 3)
	50 μM	49 ± 12% (n = 16)	22 ± 10% (n = 4)*	20 ± 6% (n = 4)*	9.7 ± 7.4% (n = 5)*
	500 μM	77 ± 5.2% (n = 3)	46 ± 7.3% (n = 6)*	60 ± 7% (n = 3)	22 ± 4.8% (n = 3)*
		k_{-1} (s ⁻¹)			
Dev	50 μM	0.033 ± 0.0032 (n = 29)	0.032 ± 0.003 (n = 3)	0.031 ± 0.01 (n = 6)	0.044 ± 0.022 (n = 5)
	500 μM	0.027 ± 0.009 (n = 3)	0.035 ± 0.01 (n = 6)	0.025 ± 0.005 (n = 3)	0.02 ± 0.005 (n = 3)
		τ_{rec} (s)			
	500 μM	69 ± 16 (n = 3)	66 ± 22 (n = 3)	75 ± 20 (n = 4)	76 ± 12 (n = 3)

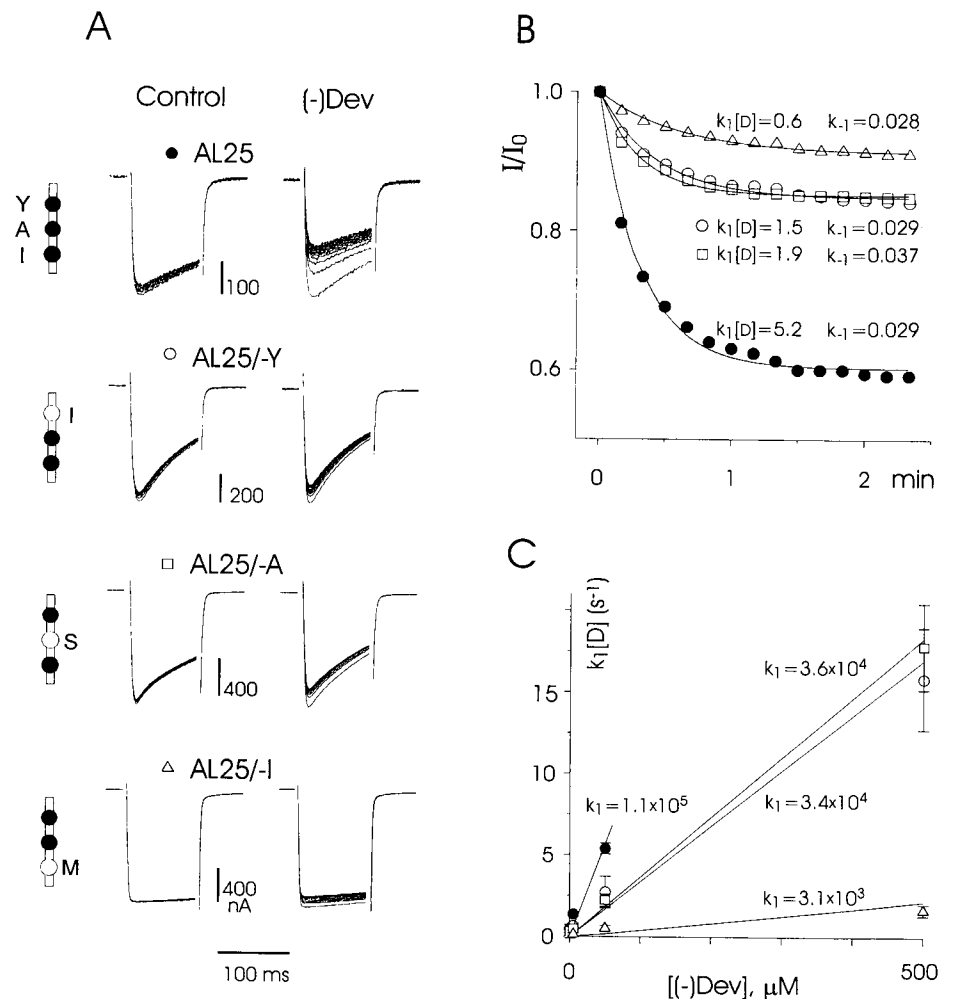
Conditioned block of I_{Ba} by (-)devapamil (5 μM, 50 μM, and 500 μM) was measured during trains of 15 consecutive depolarizing voltage pulses (100 ms, 0.1 Hz). Values are given as mean ±SD (n, number of experiments).

*Significant differences in current inhibition compared to the mutant channel AL25 ($p < 0.05$).

parent drug association rate constants for different (-)devapamil concentrations are shown in Fig. 3 C. Linear regression of the concentration-dependent first-order association rate yielded second-order association rate constants for the

channel mutants. Mutant AL25, carrying three amino acids of the putative PAA receptor site, displayed the highest sensitivity to (-)devapamil ($K_1 = 1.1 \times 10^5 \text{ M}^{-1} \text{ s}^{-1}$), whereas the single amino acid substitutions Y1804I (AL25/-Y,

FIGURE 3 I_{Ba} block by (-)devapamil in mutants AL25, AL25/-Y, AL25/-A, and AL25/-I. (A) I_{Ba} were elicited by 100-ms pulse trains from -80 mV to 20 mV (0.1 Hz) in the absence and presence of 50 μM (-)devapamil. High-affinity determinant amino acids of the L-type PAA receptor site transferred to the class A Ca²⁺ channel are schematically indicated in single-letter code (Y, A, I) as filled circles; corresponding class A amino acids are represented by white circles. (B) Time courses of peak current inhibition (same experiments as shown in A) of AL25 (●), AL25/-Y (○), AL25/-A (□), and AL25/-I (Δ) with estimated apparent drug association and dissociation rate constants (in s⁻¹). (C) Apparent association rate constants at different (-)devapamil concentrations fitted by a linear regression. Estimated second-order association rates (in M⁻¹ s⁻¹) are indicated.



$K_1 = 3.4 \times 10^4 \text{ M}^{-1} \text{ s}^{-1}$) and A1808S (AL25/-A, $K_1 = 3.6 \times 10^4 \text{ M}^{-1} \text{ s}^{-1}$) decreased the apparent drug association rate about threefold. Substitution I1811M (AL25/-I, $K_1 = 3.1 \times 10^3 \text{ M}^{-1} \text{ s}^{-1}$) induced a 30-fold decrease in the apparent PAA association rates.

Enhanced Ca^{2+} channel inactivation does not promote PAA sensitivity of class A/L-type chimeras lacking the high-affinity PAA determinants in IVS6

In a previous study we have shown that transfer of the three high-affinity PAA determinants (Hockerman et al., 1995) from L-type α_1 to the P/Q-type α_{1A} subunit enhances not only PAA sensitivity, but induces a substantial acceleration in I_{Ba} inactivation of the resulting mutants (Hering et al., 1996). Transfer of an additional L-type residue to segment IVS6 of α_{1A} (mutation F1805M; Hering et al., 1996) again attenuated both PAA sensitivity and current inactivation kinetics of the resulting quadruple mutant AL25/M (Hering et al., 1996). Furthermore, as shown in Fig. 3 A, the most remarkable reduction in PAA sensitivity was observed in mutant AL25/-I, displaying the slowest inactivation time course.

To test if Ca^{2+} channel inactivation determines the PAA sensitivity of α_{1A} in a manner that is independent of a high-affinity interaction with its receptor site, we designed

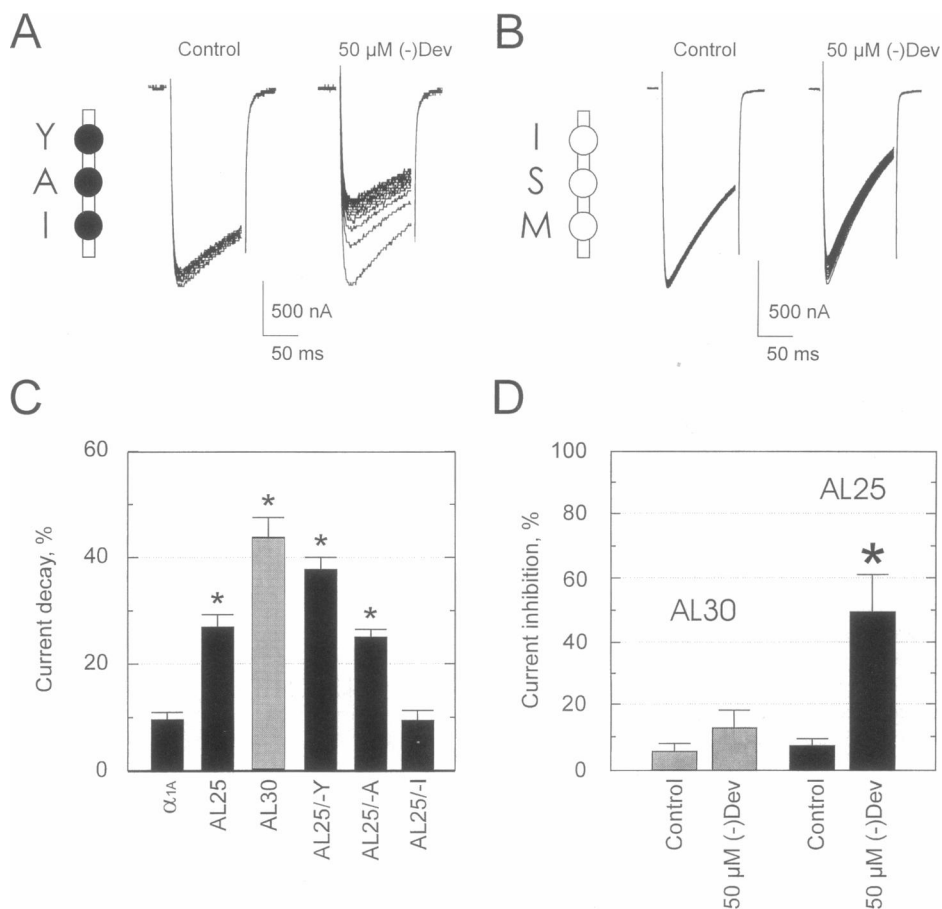
mutant AL30, which does not carry the high-affinity PAA determinants (see Materials and Methods) but inactivates at a significantly faster rate than the wild-type α_{1A} . As shown in Fig. 4, despite its significantly faster inactivation kinetics, PAA sensitivity of AL30 (estimated as use-dependent block by $50 \mu\text{M}$ D888) was comparable to the sensitivity of the low sensitive α_{1A} subunit (see also Döring et al., 1996). However, a direct comparison of the rapidly inactivating AL30 with the highly PAA-sensitive chimeras AL25, AL25/M, and AL25/-Y, M (Hering et al., 1996) reveals that accelerated current inactivation per se does not introduce a higher PAA sensitivity into the α_{1A} subunit (Fig. 4).

Different affinities of AL25, AL25/-Y, AL25/-A, and AL25/-I for (-)devapamil were also evident from different drug-induced open-channel block, resulting in an acceleration of current decay (Fig. 5). Whereas high concentrations of (-)devapamil ($500 \mu\text{M}$) caused a prominent acceleration in I_{Ba} decay in AL25 and AL25/-A, effects on I_{Ba} of AL25/-Y and AL25/-I were small or hardly detectable (Fig. 5).

Molecular determinants of the PAA receptor site in transmembrane segment IVS6 do not affect the apparent dissociation rate constants

As shown in Table 3, apparent (-)devapamil dissociation rates were not significantly affected by point mutations of

FIGURE 4 Ca^{2+} channel inactivation does not promote the PAA sensitivity of class A/L-type chimeras lacking the high-affinity PAA determinants in segment IVS6. (A, B) I_{Ba} of mutants AL25 (A) and AL30 (B) during a 0.1-Hz pulse train in controls and in the presence of $50 \mu\text{M}$ (-)devapamil. Note the faster inactivation time course of AL30 compared to AL25 shown in A. (C) Comparison of I_{Ba} inactivation of chimera AL30 with wild-type class A (α_{1A}), AL25, AL25/-Y, AL25/-A, and AL25/-I (data for α_{1A} , AL25, AL25/-Y, AL25/-A, and AL25/-I are from Hering et al., 1996), measured as I_{Ba} decay during a 100-ms test pulse from -80 mV to 20 mV . Statistical significant acceleration of current inactivation compared to class A channel I_{Ba} ($p < 0.01$) is indicated by asterisks ($n = 4-9$). (D) Use-dependent peak I_{Ba} inhibition of AL30 by $50 \mu\text{M}$ (-)devapamil (grey columns) and AL25 (black columns) during 15 depolarizing pulses from -80 mV to 20 mV (mean \pm SEM, $n = 3$) compared to current inhibition in the absence of drug (control). Statistical significance of I_{Ba} block compared to control ($p < 0.01$) is indicated by asterisks.



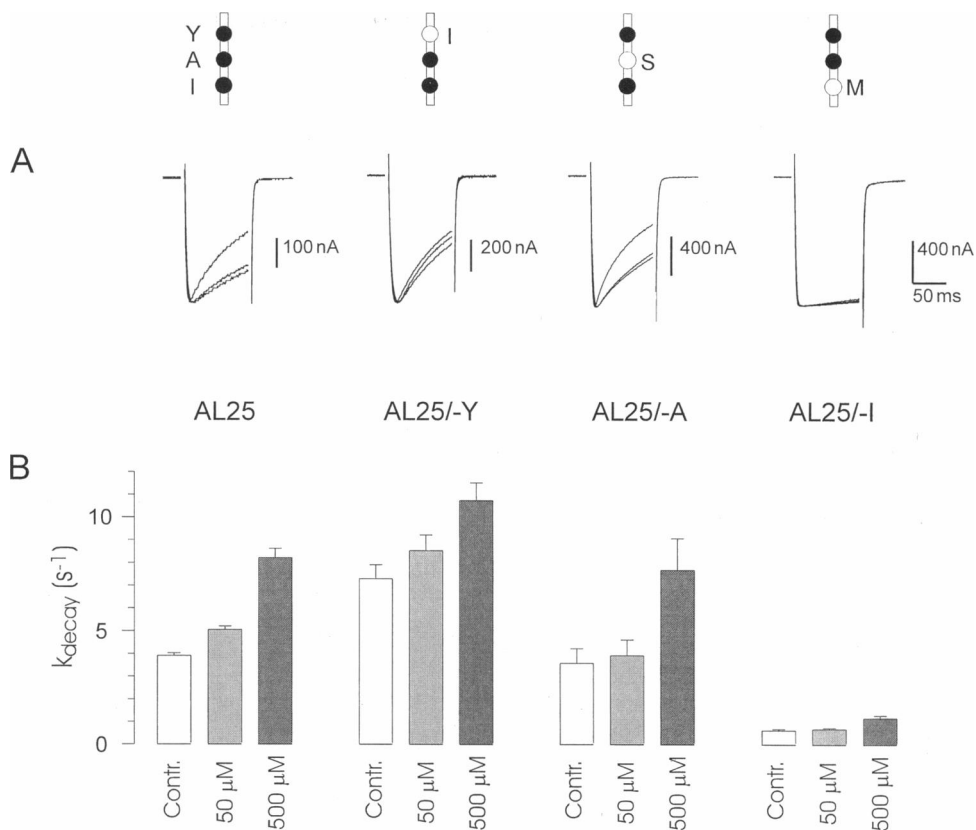


FIGURE 5 Acceleration of I_{Ba} decay by (-)devapamil. (A) Current traces (mutants AL25, AL25-Y, AL25/-A, AL25/-I) during depolarizations from -80 to 20 mV in controls and after cumulative application of 50 μM and 500 μM (-)devapamil. I_{Ba} were scaled to display drug-induced changes in current decay. (B) The mean values of I_{Ba} decay rate (k_{decay}) in control and drug, determined by means of monoexponential fit of the descending phases of I_{Ba} : $I_{\text{Ba, decay}} = A * \exp(-t * k_{\text{decay}})$ during a 100-ms pulse.

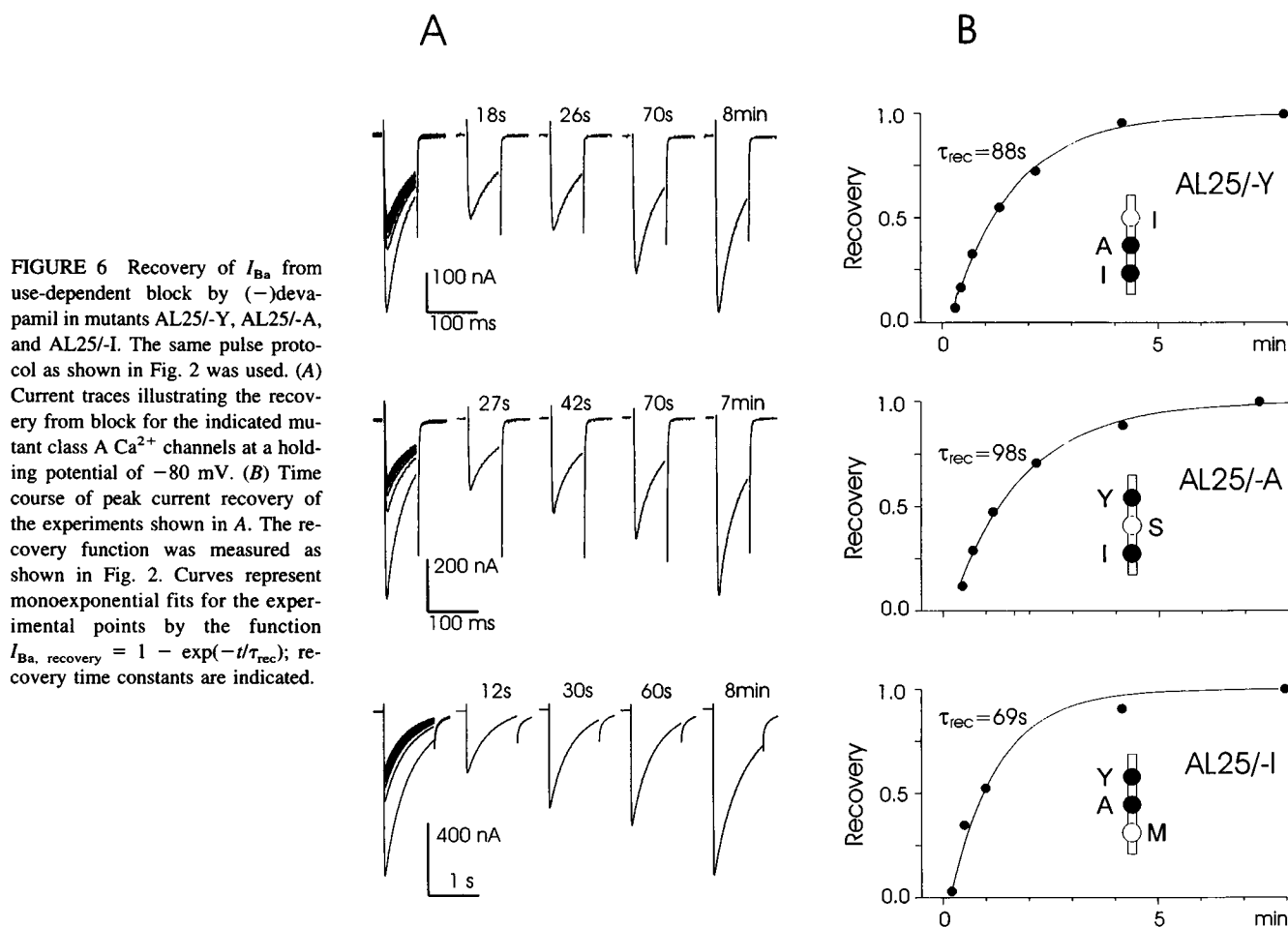
the putative PAA receptor site, as would be expected from alterations in the amino acid composition of the binding domain. This striking result prompted us to examine the recovery of resting Ca²⁺ channels from block at -80 mV by measuring peak currents at different intervals after a conditioning pulse train. A high concentration of (-)devapamil (500 μM) was applied to induce substantial channel block in the mutants AL25-Y, AL25/-A, and AL25/-I, which display a reduced PAA sensitivity compared to AL25. The time course of I_{Ba} recovery from use-dependent block by 500 μM (-)devapamil and corresponding current traces of mutants are illustrated in Fig. 6 (pulse protocol as in Fig. 2). Like the (-)devapamil dissociation rate constant, the recovery time constants from block at rest were not significantly affected by the removal of single L-type amino acid determinants of the PAA receptor site (Table 3).

Amino acids crucial for PAA action are pore orientated

The estimation of apparent drug association and dissociation rate constants is based on the assumption that PAAs interact with a receptor site that is located within the channel pore and is accessible only via the open Ca²⁺ channel conformation. During the present study we obtained independent lines of evidence confirming a high-affinity interaction of (-)devapamil with putatively pore-oriented amino acids of chimera L_h and the α_{1A} triple mutant AL25.

First, the permanently charged quaternary (-)devapamil derivative (-)q-devapamil induced use-dependent I_{Ba} inhibition. Because of its permanent charge, (-)q-devapamil is expected to access its binding domain within the channel pore exclusively via a hydrophilic pathway. As previously shown for the quaternary gallopamil (D890) in wild-type Ca²⁺ channels (Hescheler et al., 1982), (-)q-devapamil efficiently blocked Ca²⁺ channels of L_h and AL25 when applied to the intracellular side of the membrane. Fig. 7 shows I_{Ba} of L_h and AL25 during a train of 15 depolarizing test pulses (100 ms, 0.1 Hz) applied 5 min after microinjection of 50 nl (-)q-devapamil (1 mM) into the cytoplasm of a *Xenopus* oocyte (corresponding to an intracellular concentration of ~100 μM ; see Materials and Methods), compared to currents measured by the same pulse protocol in an oocyte of the same batch in drug-free solution. When 100 μM (-)q-devapamil was applied to the extracellular site, the same pulse protocol induced only weak I_{Ba} block in L_h and AL25 (Fig. 7). The amount of I_{Ba} inhibition during a pulse train by intracellularly applied (-)q-devapamil was comparable to use-dependent block by tertiary (-)devapamil (compare traces in Fig. 7 with cumulative current inhibition in the presence of 50 μM (-)devapamil in Fig. 1).

Second, I_{Ba} inactivation was not a precondition for channel block by (-)devapamil. This could be clearly demonstrated for mutant AL25, where long-lasting depolarizations of the membrane in the presence of 50 μM (-)devapamil



did not significantly ($p > 0.05$) affect the availability of Ca^{2+} channels of AL25 ($V_{0.5, control} = -19 \pm 2$ mV, $V_{0.5, drug} = -20 \pm 2$ mV, $n = 4$, Fig. 8 A). We observed,

however, some changes in the voltage dependence of Ca^{2+} channel availability in similar experiments with L_h : $V_{0.5, control} = -26 \pm 4$ mV versus $V_{0.5, drug} = -34 \pm 6$ mV,

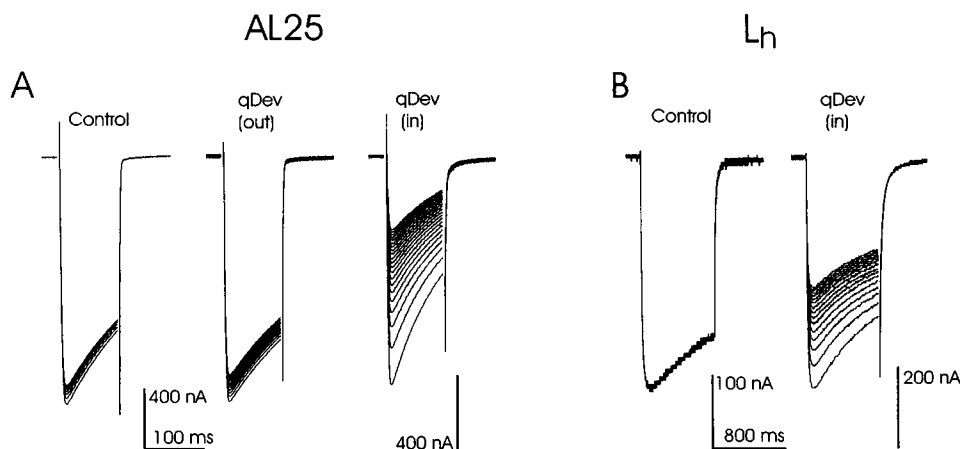


FIGURE 7 Action of the permanently charged quarternary (-)devapamil derivative q(-)devapamil on the I_{Ba} of chimera L_h and mutant AL25. (A) I_{Ba} of AL25 elicited by 100-ms pulses applied at 0.1 Hz from -80 to 20 mV in controls and after extracellular (out, $50 \mu M$) or intracellular (in, $\sim 100 \mu M$; see Materials and Methods) application of (-)q-devapamil. Control currents and currents measured during a train after extracellular application of (-)q-devapamil are from a different oocyte than currents measured after microinjection of the drug. (B) I_{Ba} of chimera L_h elicited by a train of 800-ms test pulses (0.1 Hz) from -80 to 20 mV in a control oocyte and after intracellular application of $\sim 100 \mu M$ (-)q-devapamil. Extracellular application of $100 \mu M$ (-)q-devapamil did not induce significant peak current inhibition in L_h (data not shown).

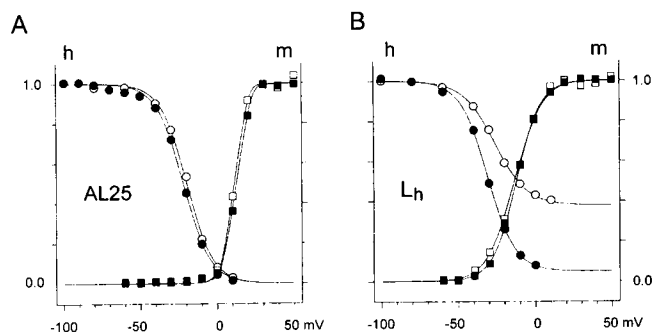


FIGURE 8 Availability (○, control; ●, in 50 μM (-)devapamil) and activation (□, control; ■, in 50 μM (-)devapamil) curves of the mutant AL25 (A) and chimera L_h (B). Activation was measured as $m = g_{\text{peak}}/g_{\text{peak, max}}$, where $g_{\text{peak}} = I_{\text{peak}}/(E - E_{\text{rev}})$, $g_{\text{peak, max}}$, maximum value of g_{peak} , measured on the descending phase of the current-voltage relationship. Availability (h) was estimated from normalized peak I_{Ba} during a 50-ms test pulse after the 10-s conditioning prepulse of a given voltage. The interpulse interval was 3 ms. Conditioning and test pulses were applied every 60 s from a holding potential of -100 mV. Curves are drawn according to the equation $I/I_{\text{max}} = I_{\text{ss}} + (1 - I_{\text{ss}})/(1 + \exp[(V - V_{0.5})/k])$.

$I_{\text{ss, control}} = 0.38 \pm 0.05$ versus $I_{\text{ss, control}} = 0.05 \pm 0.03$, $k_{\text{control}} = 9.9 \pm 0.8$ mV versus $k_{\text{drug}} = 8.6 \pm 0.3$ mV, $n = 3$ ($p < 0.05$) (Fig. 8 B). Neither the midpoint voltage I_{Ba} activation of L_h ($V_{0.5, \text{control}} = -16.5 \pm 7$ mV versus $V_{0.5, \text{drug}} = -16 \pm 5$ mV) nor that of AL25 ($V_{0.5, \text{control}} = 10 \pm 3$ mV versus $V_{0.5, \text{drug}} = 7 \pm 2$ mV, $n = 3$) was significantly affected by 50 μM (-)D888.

In contrast to the high-affinity interaction of L-type Ca²⁺ channels with antagonist 1,4-dihydropyridines (Bean, 1984), resulting in a pronounced shift in the midpoint voltage of the Ca²⁺ channel availability curve (Hering et al., 1993), the PAA-induced shift was not significant for AL25 or for the L-type chimera L_h ($p > 0.05$). Our data confirm that PAA-induced block does not occur at voltages below the threshold of channel activation (see corresponding activation curves in Fig. 8) and requires the open state (Lee and Tsien, 1983; McDonald et al., 1984; Hering et al., 1989). However, our results do not exclude the possibility that channel inactivation that occurs after drug interaction with its high-affinity receptor site could play a role in the stabilization of a nonconducting channel conformation (Nawrath and Wegener, 1997). The reduction of the “non-inactivating” current component (I_{ss}) and changes in the slope (k) of the fitted Boltzman function can hardly be attributed to a shift and scaling of the availability curve, as predicted for a high-affinity interaction of a drug with closed inactivated Ca²⁺ channels. Drug-induced deviations in the shape of the availability curve of L_h were correlated with the activation curve (Fig. 8 B) and more likely result from an open-state-dependent block than from (-)devapamil interaction with inactivated channels (see Hering and Timin, 1993, for detailed theoretical analysis).

DISCUSSION

Kinetics of state-dependent Ca²⁺ channel inhibition by Ca²⁺ antagonists (e.g., PAAs) during repeated depolarizations can be characterized by the peak current inhibition during a pulse train and the time constant of block development. Both parameters are strongly dependent on the experimental conditions, such as pulse length and frequency of stimulation (see Fig. 1). These indices make it possible to compare different drug affinities for a given channel population if a standard pulse protocol is used. The availability of cloned Ca²⁺ channels and the recent identification of the high-affinity determinants of the PAA receptor site provide the means for a detailed mutational analysis of PAA-Ca²⁺ channel interaction (Hockerman et al., 1995; Döring et al., 1996; Hering et al., 1996). Swapping of sequences between different channel types as well as single point mutations are often accompanied by changes in current kinetics. Applied pulse protocols have to be adapted for a given channel construct, thereby complicating a direct comparison of drug affinities in terms of the parameters mentioned above. Therefore, we made use of a technique for estimation of apparent association and dissociation rate constants that does not depend on the applied pulse protocols (see Timin and Hering, 1992).

Sequence environment of PAA receptor site affects the apparent association and dissociation rate constants of (-)devapamil

Our results revealed a substantial modulation of the PAA-Ca²⁺ channel interaction by the sequence environment of the putative receptor site. The apparent drug association rates of mutant AL25 exceeded those of the L-type chimera L_h by ~5 times (Table 1). The same effect was evident from the time courses of block development in L_h and AL25 shown in Fig. 1. Hence identical pulse protocols always induced a faster block development in mutant AL25.

Apparent dissociation rates estimated from the current decay during a given train of pulses (Table 1) slightly exceeded those obtained from recovery measurements (Fig. 2). To a first approximation, we estimated an “averaged” apparent dissociation rate from open and resting channels. Consequently, dissociation rates estimated from pulse train experiments will exceed the rate of recovery from block at -80 mV holding potential where Ca²⁺ channels are exclusively in a closed resting conformation (Table 1, Fig. 2). We therefore conclude that PAA dissociation from open Ca²⁺ channels might occur at significantly higher rates than from a closed-channel conformation because of drug trapping.

Point mutations of the PAA receptor site affect only the apparent association rate of (-)devapamil

Previous attempts to estimate the impact of individual amino acids on formation of the PAA receptor site in

transmembrane segment IVS6 used the steady level of current inhibition during a standard pulse train for characterization of the PAA sensitivity (Hockerman et al., 1995; Döring et al., 1996; Hering et al., 1996). We confirmed the validity of this approach by showing that a reduced sensitivity for (-)devapamil of chimeras AL25/-Y, AL25/-A, and AL25/-I was accompanied by a reduction in channel block during pulse trains compared to AL25 (Table 3).

More detailed information can be obtained from an estimation of the apparent drug association rates (Fig. 3, B and C). As expected from previous experiments with gallopamil (Hering et al., 1996), single point mutations of the PAA receptor site in AL25 reduced PAA association rates. Compared to AL25, mutants AL25/-Y and AL25/-A had an approximately threefold reduced apparent (-)devapamil association rate. Interestingly, a ~30-fold reduction was observed for mutant AL25/-I, suggesting a key role for Ile-1811 in AL25 (corresponding to Ile-1470 in α_{1C-c} ; Hockerman et al., 1995) in the formation of the PAA receptor site.

Surprisingly, the recovery of I_{Ba} from block at rest (Fig. 6) as well as the apparent dissociation rate constants estimated from train experiments (Table 3) were not significantly affected by point mutations of the putative PAA receptor site (chimeras AL25/-Y, AL25/-A, and AL25/-I). As mentioned above, we cannot exclude the possibility that drug dissociation from closed channels occurs at a significantly slower rate than from open channels. We assume that drug dissociation from the PAA receptor site in the channel pore is not rate limiting for channel unblock at rest. "Guarding" channel structures (Hille, 1977; Starmer and Grant, 1985), preventing drug access to the receptor site in closed channels, may also prevent drug escape from the channel pore in the resting state (see Qu et al., 1995, for analogous structures in sodium channels). If this energy barrier is higher than the energy required for drug dissociation from the receptor site, the resulting dissociation rate at rest would not significantly depend on the determinants of the putative receptor site.

We have shown that PAA association as well as dissociation are strongly affected by the sequence environment of the putative receptor site. Those structural elements could directly contribute binding energy for the PAA-receptor interaction, modulate the access pathway of PAAs to their receptor site, or even participate in both processes. Further progress in understanding of the molecular mechanisms of PAA interaction with Ca^{2+} channels may therefore be expected from the development of new approaches that account for individual drug dissociation rates from open and resting Ca^{2+} channels and the identification of drug access-regulating, "guarding" amino acids.

We thank Drs. Y. Mori and K. Imoto for the gift of the α_{1A} cDNA, Dr. A. Schwartz for providing the α_{1C-a} and $\alpha_{2-\delta}$ cDNA, B. Kurka and D. Kandler for expert technical assistance, and O. F. Dehtyar for help in data analysis.

We also thank Prof. H. Glossmann for critical comments on the manuscript and continuous support of our work, Dr. J. Striessnig for helpful discussions, and Dr. Traut (Knoll AG, Ludwigshafen, Germany) for providing the phenylalkylamine (-)-gallopamil.

This work was supported by grants from the Fonds zur Förderung der Wissenschaftlichen Forschung S6601 (HG) and S6603 (SH), the Dr. Legerlotz Stiftung, and the Hans und Blanca Moser Stiftung (SA).

REFERENCES

- Bean, B. P. 1984. Nitrendipine block of cardiac calcium channels: high affinity binding to the inactivated state. *Proc. Natl. Acad. Sci. USA.* 81:6388–6392.
- Birnbaumer, L., K. P. Campbell, W. A. Catterall, M. M. Harpold, F. Hofmann, W. A. Horne, Y. Mori, A. Schwartz, T. P. Snutch, T. Tanabe, and R. W. Tsien. 1994. The naming of voltage-gated calcium channels. *Neuron.* 13:505–506.
- Catterall, W. A. 1995. Structure and function of voltage-gated ion channels. *Annu. Rev. Biochem.* 64:493–531.
- Catterall, W. A., and J. Striessnig. 1992. Receptor sites for calcium antagonists. *Trends Pharmacol. Sci.* 13:256–262.
- Diochot, S., S. Richard, M. Baldy-Moulinier, J. Nargeot, and J. Valmier. 1995. Dihydropyridines, phenylalkylamines and benzothiazepines block N-, P/Q- and R-type calcium channels. *Pflügers Arch.* 431:10–19.
- Döring, F., V. E. Degtiar, M. Grabner, J. Striessnig, S. Hering, and H. Glossmann. 1996. Transfer of L-type calcium channel IVS6 segment increases phenylalkylamine sensitivity of α_{1A} (BI). *J. Biol. Chem.* 271:11745–11749.
- Dunlap, K., J. I. Luebke, and T. J. Turner. 1995. Exocytotic Ca^{2+} channels in mammalian central neurons. *Trends Neurosci.* 18:89–98.
- Glossmann, H., and J. Striessnig. 1990. Molecular properties of calcium channels. *Rev. Physiol. Biochem. Pharmacol.* 114:1–105.
- Grabner, M., K. Friedrich, H.-G. Knaus, J. Striessnig, F. Scheffauer, R. Staudinger, W. J. Koch, A. Schwartz, and H. Glossmann. 1991. Calcium channels from *Cyprinus carpio* skeletal muscle. *Proc. Natl. Acad. Sci. USA.* 88:727–731.
- Grabner, M., Z. Wang, S. Hering, J. Striessnig, and H. Glossmann. 1996. Transfer of 1,4-dihydropyridine sensitivity from L-type to class A (BI) calcium channels. *Neuron.* 16:207–218.
- Hering, S., S. Aczél, M. Grabner, F. Döring, S. Berjukow, J. Mitterdorfer, M. J. Sinnegger, J. Striessnig, V. Degtiar, Z. Wang, and H. Glossmann. 1996. Transfer of high sensitivity for benzothiazepines from L-type to class a (BI) calcium channels. *J. Biol. Chem.* 271:24471–24475.
- Hering, S., T. B. Bolton, D. J. Beech, and S. P. Lim. 1989. On the mechanism of calcium channel block by D600 in single smooth muscle cells from rabbit ear artery. *Circ. Res.* 64:928–936.
- Hering, S., A. D. Hughes, E. N. Timin, and T. B. Bolton. 1993. Modulation of calcium channels in arterial smooth muscle cells by dihydropyridine enantiomers. *J. Gen. Physiol.* 101:393–410.
- Hering, S., and E. N. Timin. 1993. Estimation of drug affinities for calcium channel conformational states. In *Molecular and Cellular Biology of Molecular Targets*. Glossmann and Striessnig, editors. Plenum Press, New York. 189–219.
- Hescheler, J., D. Pelzer, G. Trube, and W. Trautwein. 1982. Does the organic calcium channel blocker D600 act from inside or outside of the cardiac cell membrane? *Pflügers Arch.* 393:287–291.
- Hille, B. 1977. Local anesthetics: hydrophilic and hydrophobic pathways for drug-receptor reaction. *J. Gen. Physiol.* 69:497–515.
- Hockerman, G. H., B. D. Johnson, T. Scheuer, and W. A. Catterall. 1995. Molecular determinants of high affinity phenylalkylamine block of L-type calcium channels. *J. Biol. Chem.* 270:22119–22122.
- Hofmann, F., M. Biel, and V. Flockerzi. 1994. Molecular basis for Ca^{2+} channel diversity. *Annu. Rev. Neurosci.* 17:399–418.

- Horton, R. M., H. D. Hunt, S. N. Ho, J. K. Pullen, and L. R. Pease. 1989. Engineering hybrid genes without the use of restriction enzymes: gene splicing by overlap extension. *Gene*. 77:61–68.
- Ishibashi, H., A. Yatani, and N. Akaïke. 1995. Block of P-type Ca²⁺ channels in freshly dissociated rat cerebellar Purkinje neurons by diltiazem and verapamil. *Brain Res.* 695:88–91.
- Lee, K. S., and R. W. Tsien. 1983. Mechanism of calcium channel blockade by verapamil, D600, diltiazem and nitrendipine in single dialysed heart cells. *Nature*. 302:790–794.
- McDonald, T. F., D. Pelzer, and W. Trautwein. 1984. Cat ventricular muscle treated with D600: characteristics of calcium channel block and unblock. *J. Physiol. (Lond.)*. 352:217–241.
- Mikami, A., K. Imoto, T. Tanabe, T. Niidome, Y. Mori, H. Takeshima, S. Narumiya, and S. Numa. 1989. Primary structure and functional expression of the cardiac dihydropyridine-sensitive calcium channel. *Nature*. 340:230–233.
- Mori, Y., T. Friedrich, M.-S. Kim, A. Mikami, J. Nakai, P. Ruth, E. Bosse, F. Hofmann, V. Flockerzi, T. Furuichi, K. Mikoshiba, K. Imoto, T. Tanabe, and S. Numa. 1991. Primary structure and functional expression from complementary DNA of a brain calcium channel. *Nature*. 350:398–402.
- Nawrath, H., and J. W. Wegener. 1997. Kinetics and state-dependent effects of verapamil on cardiac L-type calcium channels. *Naunyn-Schmiedeberg's Arch. Pharmacol.* 355:79–86.
- Qu, Y., J. Rogers, T. Tanada, T. Scheuer, and W. A. Catterall. 1995. Molecular determinants of drug access to the receptor site for antiarrhythmic drugs in the cardiac Na⁺ channel. *Proc. Natl. Acad. Sci. USA*. 92:11839–11843.
- Sanger, F., S. Nicklen, and A. R. Coulson. 1977. DNA sequencing with chain-terminating inhibitors. *Proc. Natl. Acad. Sci. USA*. 74:5463–5467.
- Starmer, C. F., and A. O. Grant. 1985. Phasic ion channel blockade: a kinetic model and method for parameter estimation. *Mol. Pharmacol.* 28:348–356.
- Timin, E. N., and S. Hering. 1992. A method for estimation of drug affinity constants to the open conformational state of calcium channels. *Biophys. J.* 63:808–814.